Optimal reorganization of photosynthesis after the evolution of C_4

Haoran Zhou[1,2,3], Erol Akçay[1], Brent Helliker[1]

[1]Department of Biology, University of Pennsylvania, Philadelphia, PA 19104, USA

[2]School of Forestry and Environmental Studies, Yale University, New Haven, CT 06511, USA

[3]University Corporation for Atmospheric Research, Boulder, CO 80301, USA

Correspondence: Haoran Zhou

Email: haoran.zhou@yale.edu

Conflict of interest: None declared.

Abstract

The evolution of C_4 photosynthesis evolved numerous times independently in the grasses over tens of millions of years, and each event required the development of distinct biochemistry and anatomy. Recent theoretical, anatomical and phylogenetic studies made great progress in reconstructing the evolutionary processes leading to the formation of the C_4 carbon concentration mechanism (CCM) in grasses. After the formation of the full CCM, C_4 physiology continued to diverge between C_3 and C_4 grasses, presumably as selection optimized photosynthetic function. In this study, we combine optimality modeling, physiological measurements and phylogenetic analysis to examine how various aspects of C_4 photosynthetic machinery were reorganized within a lineage and as compared to closely-related C_3 grasses. Both model and empirical results support a strong, and comparatively rapid, reorganization in resource allocation between the Calvin-Benson cycle and light reactions in C_4, as determined by a higher maximal electron transport to maximal Rubisco carboxylation rate (J_{max}/V_{cmax}). Our model, chlorophyll a/b ratios, and fluorescence-based electron transport measurements all suggest that linear electron transport represents a lower proportion (approximately 67%) of total electron transport in C_4, and that the impetus for increased cyclic-electron transport is to balance ATP:NADPH stoichiometry, as opposed to decreasing O_2 in the bundle sheath cells. Finally, the tight coordination between RuBP carboxylation and PEP carboxylation occurred coincidently with the evolution of the C_4 CCM, with a relatively constant maximal PEP carboxylation rate and V_{cmax} (V_{pmax}/V_{cmax}).

Key words C_4 evolution, chlorophyll a/b, cyclic-electron transport, grass, optimal J_{max}/V_{cmax}, photosynthesis

Introduction

C_4 photosynthesis pathway evolved as a response to inefficiencies of C_3 photosynthesis that are exacerbated under certain environmental conditions (Ehleringer and Monson 1993; Ehleringer et al. 1997). Rubisco, the carboxylating enzyme of the Calvin-Benson (CB) cycle, not only assimilates CO_2, but also O_2, which is the first step in the photorespiratory pathway that reduces C_3 photosynthesis up to 30% (Ehleringer et al., 1991; Bauwe et al., 2010; Raines 2011). The C_4 pathway dramatically reduces Rubisco oxygenation, and consequently photorespiration, by concentrating CO_2 around Rubisco. This carbon concentrating mechanism (CCM) is achieved by segregating atmospheric CO_2 uptake by Phosphoenolpyruvate carboxylase (PEPc) and CB-cycle

CO_2 assimilation by Rubisco into two compartments within the leaf. In the mesophyll cells, carbonic anhydrase hydrates CO_2 and then PEPc catalyzes HCO_3^- and PEP into C_4 acids. The C_4 acids are transported to the bundle sheath cells that surround leaf veins, in a configuration called Kranz anatomy in most C_4 species. In the bundle sheath cells, C_4 acids are decarboxylated to create a high CO_2 environment for the Rubisco, and PEP is regenerated and translocated back to the mesophyll cells (Hatch & Osmond, 1976; Kellogg, 1999). The bundle sheath is often constructed in a manner that lessens the leakiness of CO_2 to the mesophyll, an anatomical phenomenon that enhances the efficiency of C_4 pathway (Brown and Byrd 1993; Ubierna et al. 2013; Kromdijk et al. 2014). Meanwhile, the regeneration of PEP requires ATP, so the C_4 CCM has an energetic cost that is not required by C_3 photosynthesis (Hatch, 1987).

The assembly of the full C_4 CCM is thought to have occurred through intermediate steps of selective advantage (Sage, 2001, 2004, 2018; Christin & Osborne, 2014; Lundgren,2019). It is thought that the anatomical precursors of C_4 evolution were the enlargement of the vascular bundle sheath and a decrease of inter-veinal distance, termed the proto-Kranz condition (McKown & Dengler, 2007; Christin et al., 2013a; Griffiths et al., 2013). Then, a C_2 cycle evolved in which photorespired CO_2 is recovered and concentrated in the bundle sheath (Sage et al., 2012; Mallmann et al., 2014). Along with the evolution of the C_2 cycle, the mesophyll to bundle sheath ratio was reduced further. The enzymes related to the CCM function exists in the C_3 pathway and the citric-acid cycle, and spatially explicit expression of these enzymes led to the establishment of the full C_4 cycle (Aubry et al., 2011; Christin et al., 2013b). However, after the formation of the full CCM, C_4 physiology continued to diverge between C_3 and C_4 species, presumably as selection optimized the function of the CCM within a given ecological niche (Christin and Osborne, 2014; Sage, 2016). Zhou et al. (2018) and Zhou (2020) discussed the potential reorganization of hydraulic systems after C_4 evolved within a grass lineage, and here we examine how various aspects of C_4 photosynthetic machinery— nitrogen allocation between the Calvin-Benson cycle and the light reactions, electron transport, and the coordination of Rubisco, electron transport and PEP carboxylation— were reorganized within a C_4 lineage and as compared to closely-related C_3 grasses.

Resource allocation (mainly nitrogen) between the CB cycle and the light reactions would likely change between C_3 and C_4 due to the formation of the CCM. The CCM concentrates CO_2 around the CB-cycle, thus allowing for less investment in nitrogen-rich Rubisco as compared to a C_3

plant, but additional ATP from the light reactions is required to maintain the CCM (Hatch, 1987). Thus, the evolution of the full CCM changes the balance between nitrogen investment in the CB cycle versus the light reactions. The resource allocation between the CB cycle and the light reactions can be represented by the ratio of maximal electron transport to maximal Rubisco carboxylation rate (J_{max}/V_{cmax}). Although J_{max}/V_{cmax} has been empirically measured in numerous C_3 species (Wullschleger, 1993) and optimal J_{max}/V_{cmax} has been modeled for C_3 (Walker et al., 2014; Kromdijk and Long, 2016; Quebbeman and Ramirez, 2016), there have been few measurements in C_4, and we are not aware of any theoretical optimality predictions. For C_4 species, the assimilation rate would be mostly limited by the light reactions (Baker and Long, 1988; Pearcy and Ehleringer, 1984; Collatz et al., 2992) and there would be a redundancy in RuBP carboxylation if a C_3-like J_{max}/V_{cmax} was maintained (Zhou et al., 2018). Furthermore, Zhou et al. (2018) showed that if nitrogen is reallocated from the CB cycle to the light reactions, which results in a higher J_{max}/V_{cmax}, C_4 assimilation rates will increase significantly in almost all environmental conditions. In C_3 plants, J_{max}/V_{cmax} should vary along with different environmental factors (temperature, CO_2, light, and water availability; Onoda et al., 2005; Rodriguez-Calcerrada et al., 2008; Kromdijk and Long, 2016; Yin et al., 2018), and we expect the same for C_4. How optimal J_{max}/V_{cmax} varies with environment would be helpful in predicting the acclimation of C_3 and C_4 to different habitats and a changing climate, especially in bio-geographical, bio-geochemical and vegetation models (Beerling and Quick, 1995; Quebbeman and Ramirez, 2016).

The C_4 CCM requires additional ATP; how and where this ATP is produced should affect the efficiency of the CCM. The primary electron transport process to generate ATP and NADPH necessary to run the CB cycle is the O_2-producing, linear electron transport through both PSI and PSII. There are two potential reasons that the balance of linear electron transport in C_4 species would be altered. The first is to balance the stoichiometry of ATP and NADPH. The extra NADPH is not required for the CCM, and can be a harmful byproduct (Kramer and Evans, 2011; Yin and Struik, 2018). Second, the extra O_2 produced could lessen the efficiency of the CCM by increasing O_2 around Rubisco (Yin et al., 2011; von Caemmerer and Furbank, 2016). Thus, enhanced cyclic-electron transport, which produces ATP only, has been proposed to play a crucial role in driving the energy requirements in the bundle sheath cells (Takabayashi et al., 2005; Munekage, 2016; Munekage and Taniguchi, 2016; Yin and Struik, 2018). Changes in the balance of linear and cyclic electron transport would be accompanied with predictable variation

in other traits. These electron-transport pathways have different association with PSI and PSII, and PSI has a higher concentration of chlorophyll a compared to chlorophyll b than PSII. Therefore, C_4 species should have a higher chlorophyll a/b ratio (Takabayashi et al., 2005), if cyclic electron transport is elevated. Also, electron transport estimates based on fluorescence measures electron transport associated with PSII in C_4 species. We propose the ratio of electron transport estimated from fluorescence (ETR) to J_{max} should be relatively low in C_4 species as compared to C_3 species. Establishing this ratio will allow for better estimation of J_{max} from fluorescence measurements in C_4 species.

The operation of CB cycle, electron transport and the CCM should be coordinated to optimize the efficiency of C_4 photosynthesis (von Caemmerer and Furbank, 2016). The PEP carboxylation process and RuBP carboxylation work in tandem to capture the CO_2. A separate aspect of C_4 coordination is that both RuBP regeneration and PEP regeneration use ATP from electron transport and provide reaction substrates for the CB cycle and PEP carboxylation, which provides. Such coordination among CB cycle, electron transport, and the CCM could be represented by the relationships among V_{cmax}, J_{max} and maximal PEP carboxylation rate (V_{pmax}). As a relationship between J_{max} and V_{cmax} has been discussed above, to depict a complete picture of the functional coordination, maximal PEP carboxylation rate to V_{cmax} (V_{pmax}/V_{cmax}) should be taken into consideration (Yin et al., 2016).

Because of the importance of testing physiological differences between species within a phylogenetic context (Edwards et al., 2007; Cavender-Bares et al., 2009), we use phylogenetic comparative methods and evolutionary models to examine the reorganization of the photosynthetic system after the evolution of C_4 across a phylogeny of C_3 and C_4 grasses from the PACMAD clade. We used both optimality modeling and physiological measurements to test the following hypotheses: (1) There will be a reorganization in resource allocation between the CB cycle and light reactions in C_4; specifically, C_4 will have a higher J_{max}/V_{cmax} to maximize the assimilation rate. (2) The electron-transport rate to J_{max} ratio (ETR/J_{max}) is lower, and chlorophyll a/b ratios higher, in C_4 species. (3) The enhanced cyclic-electron transport aims to balance the stoichiometry of ATP and NADPH, as well as to decrease O_2 accumulation in the bundle sheath. (4) The coordination of RuBP carboxylation by Rubisco, electron transport and PEPc carboxylation of PEP result in relatively constant V_{pmax}/V_{cmax} to maximize assimilation

rate. Lastly, a better formal understanding of how J_{max}/V_{cmax} and V_{pmax}/V_{cmax} vary in C_4 species will provide important input parameters for large-scale models to predict the carbon/nitrogen cycle, vegetation dynamics and productivity.

Materials and Methods

Plant material

We cultivated 36 closely related species, including nine C_3, 26 C_4 species in three C_4 subtypes and one intermediate species selected from Grass Phylogeny Working Group II, (2012). We, then, extracted the dated phylogenetic tree for the species from the dated phylogenetic trees (Spriggs et al., 2014). C_4 species belong to three C_4 subtypes and could be classified as nine closely-related C_3 and C_4 Clusters. Detailed cultivation and phylogeny information is the same as Zhou (2020).

Physiological Modeling

Optimal J_{max}/V_{cmax} and V_{pmax}/V_{cmax} We used the model of Zhou et al. (2018), which incorporates the soil-plant-air water continuum into traditional C_3 and C_4 photosynthesis models and optimizes stomatal resistance and leaf/fine-root allocation to maximize total carbon gain, to get predictions of the further evolution and reorganization of photosynthetic systems. Using such a framework, we can model the optimal J_{max}/V_{cmax} and V_{pmax}/V_{cmax} considering the following nitrogen stoichiometry:

The total nitrogen is the sum of different components (Evans, 1989a):

$$N_{org} = N_P + N_E + N_R + N_S + N_O, \quad (1)$$

in which N_P represents the nitrogen in pigment proteins, N_E represents the nitrogen for the electron transport system, N_R represents the nitrogen of Rubisco, N_S represents nitrogen in soluble proteins except for Rubisco, and N_O represents additional organic leaf nitrogen not invested in photosynthetic functions.

In order to model the optimal J_{max}/V_{cmax} and V_{pmax}/V_{cmax}, we need to consider the nitrogen stoichiometry among J_{max}, V_{cmax} and V_{pmax}. We used empirical relationships found in previous studies (Evans and Poorter, 2001; Niinemets and Tenhunen, 1997; Quebbeman and Ramirez, 2016):

$$N_P + N_E = 0.079J_{max} + 0.0331\chi, \quad (2)$$

$$N_S = \nu J_{max}, \quad (3)$$

$$N_R = V_{cmax}/(6.25 \times V_{cr} \times \xi), \quad (4)$$

$$N_{PEP} = V_{pmax}/(6.72 \times V_{pr} \times \xi), \quad (5)$$

χ is the concentration of chlorophyll per unit area (μmol Chl m^{-2}), 0.079 is in mmol N s $(\mu mol)^{-1}$, and 0.0331 is in mmol N $(\mu mol\ Chl)^{-1}$, $\nu \approx 0.3$ (mmol N s $(\mu\ mol)^{-1}$. V_{cr} is the specific activity of Rubisco (the maximum rate of RuBP carboxylation per unit Rubisco; ≈ 20.5 μmol CO_2 (g Rubisco)$^{-1}s^{-1}$) and 6.25 is grams RuBisCO per gram nitrogen in RuBisCO. V_{pr} is the specific activity of PEPc, that is, the maximum rate of RuBP carboxylation per unit PEPc (≈ 181.7 μmol CO_2 (g PEPC)$^{-1}s^{-1}$) (Supplementary Material I), 6.72 is grams PEPc per gram nitrogen in PEPC (calculated from the amino acids composition of Fujita et al., 1984), and ξ is the mass in grams of one millimole of nitrogen equal to 0.014 g N (mmol N)$^{-1}$.

Further, we simplify the equation (2) by assuming there is a coordination of resource allocation between chlorophyll and electron transport for saturated light intensity, which determines the J_{max}. We make this assumption for the light saturated condition and use the empirical equation of Croft et al. (2017) to equation (2)

$$\chi = \frac{1000J_{max}}{2.49}/\eta, \quad (6)$$

where η is the average molar mass for chlorophyll (900 g/mol). Thus,

$$N_{org} - N_O = 0.079J_{max} + 0.0331\chi + \nu J_{max} + \frac{V_{cmax}}{6.25 \times V_{cr} \times \xi} + V_{pmax}/(6.72 \times V_{pr} \times \xi), \quad (7)$$

When the light intensity varies, the following function is used to adjust the electron transport rate (Ögren and Evans, 1993):

$$J = \frac{I_2 + J_{max} - \sqrt{(I_2 + J_{max})^2 - 4\Theta I_2 J_{max}}}{2\Theta}. \quad (8)$$

Also, all the photosynthetic parameters are temperature-sensitive (Zhou et al., 2018).

In the optimal modeling processes for C_4 pathway, we set N_{org}- N_O as constant of 129 mmol N m^{-2} (which yield a V_{cmax}= 39 μmol m^{-2} s^{-1}, J_{max}= 195 μmol m^{-2} $s^{-1}$and V_{pmax}= 78 μmol m^{-2} s^{-1}, assuming J_{max}/V_{cmax}=5 and V_{pmax}/V_{cmax}=2) and model the assimilation rates with different J_{max}/V_{cmax} from 1 to 8 of 0.01 interval by maintaining V_{pmax}/V_{cmax}=2, which is the empirically

measured average in our study. Then, we model the assimilation rates with different V_{pmax}/V_{cmax} from 0.5 to 6 of 0.01 interval under J_{max}/V_{cmax}=5, which is also the empirical average in our measurements. The corresponding J_{max}/V_{cmax} or J_{max}/V_{cmax} under the highest assimilation rates represent the optimal ratios. Using the model described above, we were able to model the optimal J_{max}/V_{cmax} and V_{pmax}/V_{cmax} under different environmental gradients: CO_2 of 200, 300, 400, 500 and 600 ppm; VPD and ψ_S of (0 MPa, 0.15) (0.625, -0.5), (1.25, -1), (1.875, -1.5), and (2.5, -2); light intensity of 2000, 1600, 1200, 800 and 400 $\mu mol m^{-2} s^{-1}$; temperature of 15, 20, 25, 30 and 35 ^{o}C. Since there is uncertainty for relationships, we performed sensitivity analysis for the total nitrogen (from 100% to 50% with 10% interval of the regular nitrogen) for optimal J_{max}/V_{cmax} and V_{pmax}/V_{cmax} results and we also performed sensitivity analysis for stoichiometry of PEPC by varying the $1/(6.72\times V_{pr} \times \xi)$ term in Eq. 5 from 50% to 800%. For the C_3 pathway, all the modeling process are similar with the C_4 and a same value of N_{org}- N_O is used, except that a simplified version of equation (7) is used as below (Quebbeman and Ramirez, 2016):

$$N_{org} - N_O = 0.079J_{max} + 0.0331\chi + \nu J_{max} + \frac{V_{cmax}}{6.25\times V_{cr}\times \xi}, \quad (9)$$

Effects of decreasing V_{cmax} Using the model, we also simulated the effect of decreasing V_{cmax} on the assimilation rate of C_4 pathway. In this modeling process, we hold J_{max} and other photosynthetic parameters constant as the initial modeling condition as above, but varying the V_{cmax} to 100%, 90%, 80%, 70%, 60% and 50% of the original values of C_3.

Effects of O_2 evolution in bundle sheath We used the C_4 photosynthesis model to model the effects of different proportion of O_2 evolution (indicated by α) in bundle sheath on assimilation rate (von Caemmerer, 2000; Yin et al., 2011). The modeling conditions are α=0, 0.15, 0.5 and 1. A detailed description of the model could be found Zhou et al. (2019).

Gas exchange and fluorescence measurements

We measured A/C_i curves using a LI-6400XT (LI-COR Inc., Lincoln, NE, USA) for all the species by setting the CO_2 concentrations as 400, 200, 50, 75, 100, 125, 150, 175, 200, 225, 250, 275, 300, 325, 350, 400, 500, 600, 700, 800, 1000, 1200, 1400 ppm under light intensity of 2000 $\mu mol m^{-2} s^{-1}$. Data were recorded when the intercellular CO_2 concentration equilibrated 2-5 minutes. Fluorescence was measured along with A/C_i curves using a 2 cm^2 fluorescence chamber

head. After the change of CO_2 concentration, the quantum yield was measured by multiphase flash when A reached a steady state (Bellasio et al. 2014). The leaf temperatures were controlled at 25°C, VPD varied at 1-1.7kPa and the flow rate of 500 μmol s^{-1} for all the measurements. The cuvette was covered by Fun-Tak to lessen leakiness. The A/C_i curves were used to estimate V_{cmax}, J_{max}, and V_{pmax} using Zhou et al. (2019). Fluorescence results were used to calculate the ETR (Genty et al., 1989).

Chlorophyll measurements and leaf nitrogen

Chlorophyll a and b were measured using the spectrophotometer method (Porra et al., 1989). We cut the fresh leaves of species into pieces of 0.5 mm long (total leaf area was measured) and submerged the fragments into DMF. After all the Chlorophyll was extracted and the leave turned white, the supernatant was used to measure the absorption under 663.8 nm and 646 nm. Calculations of Chlorophyll a and b concentrations were calculated using the equation of Porra et al. (1989). Then we measure leaf nitrogen contents for each sample using the CHNOS analyzer (ECS4010, Costech Analytical Technologies, Inc., Valencia, CA).

.

Phylogenetic analysis

We fitted each of the photosynthetic parameters (V_{cmax}, J_{max}, J_{max}/V_{cmax}, Total Chl, ETR/J_{max}, Chl a/b, ETR, V_{pmax} and V_{pmax}/V_{cmax}) to six different evolutionary models falling into Brownian Motion model and Ornstein-Uhlenbeck Model using the R package of "mvMORPH" (Table S1). The small-sample-size corrected version of Akaike information criterion (AICc, the lower AICc, the better fit) and Akaike weights (AICw, the higher AICw, the better fit) were used as criteria to figure out the best-fitted model. We used likelihood-ratio test (LRT) method to test whether one model variant performs significantly better than others. Furthermore, we used SubtypeModels to test whether there are significant differences among C_4 subtypes (Table S1). The detailed description of the evolutionary models and phylogenetic analysis can be found in Zhou (2020).

Results

As a preliminary analysis for the raw data, we conducted ANOVA tests within each phylogenetic cluster (Table 1). ANOVA tests indicated all C_4 had higher J_{max}/V_{cmax}, and Chl a/b than their

corresponding C_3 in different clusters, while C_4 had the lower V_{cmax} and ETR/J. There are no consistent relationship for J_{max}, chlorophyll concentration, and ETR between C_3 and C_4 among clusters. For nitrogen content, C_3 have higher or equivalent values than corresponding C_4. We further performed phylogenetic analysis to test our hypotheses shown as below.

C_4 species have higher J_{max}/V_{cmax} than C_3 species

The modeling results of the optimal J_{max}/V_{cmax} and empirical measurements for J_{max}/V_{cmax} are significantly higher for the C_4 species than those for the C_3 species (Fig. 1). The experimental measurements were relatively consistent with the modeling results, although measured values were slightly lower than modeled values in C_3 and C_4. C_4 species always had significantly higher J_{max}/V_{cmax} than their closely-related C_3 species (Table 1); furthermore, phylogenetic analysis shows the J_{max}/V_{cmax} follows the Ornstein-Uhlenbeck model with a higher root state for C_4 species and a lower root state for C_3 (Table 2; phylogeny is shown in Zhou (2019)). The evolutionary models differentiating subtypes did not fit significantly better than models only considering C_3 and C_4 photosynthesis types for J_{max}/V_{cmax} (Table S2, S11), which means no significant differences of J_{max}/V_{cmax} among subtypes were detected.

Table 1 The photosynthetic parameters of J_{max}/V_{cmax}, V_{cmax}, J_{max}, total Chl, ETR/J_{max}, Chl a/b, ETR and nitrogen content between closely related C_3 and C_4 species. The different blocks show nine different clusters of closely-related C_3 and C_4 species. * indicate C_3 species, † indicate C_3-C_4 intermediate species, and the rest are C_4 species. Letters indicate significant differences for the species within each cluster. The data indicate average(standard error).

Species	J_{max}/V_{cmax}	J_{max}	V_{cmax}	Tchl	ETR/J_{max}	ETR	Chl a/b	Nitrogen
S. decipiens†	1.5(0.1)a	71(4.3)a	54(3.8)a	0.36(0.03)a	1.2(0.02)a	82.4(6.4)a	3.4(0.1)ab	3.4(0.1)ab
A. rufa	4.9(0.1)b	94(6.4)b	20(1.2)b	0.37(0.03)a	0.6(0.02)b	64.6(3.7)ab	4.1(0.1)c	3.0(0.1)a
A. villosa	5.1(0.1)b	92(7.4)b	19(1.3)b	0.30(0.03)ab	0.6(0.02)b	59.2(4.9)b	4.2(0.1)c	3.5(0.1)b
*H. pernambucense**	1.5(0.1)a	59(3.3)bc	47(3.3)a	0.23(0.01)b	1.1(0.03)a	67.3(4.4)ab	3.3(0.1)b	3.6(0.1)b
*S. laxum**	1.4(0.1)a	80(4.70)c	56(3.4)a	0.29(0.03)ab	1.0(0.02)c	79.1(3.2)ab	3.5(0.1)a	4.6(0.11)c
D. dinteri	5.5(0.1)a	168(9.2)a	31(1.3)ad	0.38(0.02)a	0.6(0.01)a	100.7(5.9)a	4.8(0.1)a	3.5(0.2)a
T. superba	5.1(0.1)b	104(7.8)b	22(1.6)ab	0.37(0.02)a	0.6(0.01)a	67.8(5.9)bc	4.5(0.1)a	2.4(0.2)b
L. simplex	4.5(0.1)c	83(7.6)ab	19(1.3)b	0.38(0.04)a	0.6(0.03)a	48.5(4.3)b	4.0(0.1)b	2.2(0.1)b
*T. latifolia**	1.5(0.1)d	77(6.6)bc	54(4.4)c	0.30(0.02)a	1.0(0.04)b	72.3(7.8)c	3.5(0.1)c	4.2(0.2)a

C. latifolia[*]	1.6(0.1)d	53(4.1)c	34(2.1)d	0.30(0.02)a	1.0(0.08)b	52.5(3.0)b	3.4(0.1)c	2.3(0.1)b
Z. bulbosa	4.3(0.2)a	88(9.2)a	20(1.2)a	0.21(0.01)a	0.6(0.01)a	46.3(4.7)a	3.9(0.1)a	2.9(0.1)a
S. italica	4.6(0.1)a	75(8.1)a	17(1.5)a	0.43(0.01)b	0.7(0.03)ab	50.9(3.4)a	4.0(0.1)a	3.1(0.2)a
S. sphacelata	5.3(0.1)b	102(8.0)ac	20(1.0)a	0.35(0.04)bc	0.6(0.03)ab	64.4(3.4)a	4.1(0.1)a	3.7(0.3)ab
W. capillipes	5.7(0.1)b	147(9.8)b	27(1.4)a	0.34(0.03)bc	0.8(0.01)b	110.9(7.8)b	4.1(0.1)a	3.5(0.1)a
H. proluta[*]	1.5(0.1)c	127(8.9)bc	84(5.5)b	0.30(0.03)c	1.1(0.03)c	136.2(7.4)c	3.1(0.1)b	4.3(0.1)b
T. monachne	5.5(0.2)a	160(13.8)a	30(2.9)a	0.31(0.01)ab	0.7(0.02)a	111.0(9.3)a	3.7(0.1)a	3.9(0.3)a
E. meyeriana	5.2(0.1)ab	135(7.6)ab	26(1.3)a	0.29(0.02)ab	0.6(0.01)b	81.7(7.5)ab	3.8(0.1)a	3.6(0.2)a
M. maximus	5.1(0.1)b	117(5.5)b	24(0.9)a	0.39(0.02)b	0.6(0.02)ab	80.5(5.1)b	3.5(0.1)a	4.5(0.3)a
U. ruziziensis	5.2(0.1)ab	121(6.0)ab	23(1.1)a	0.24(0.02)a	0.6(0.02)ab	76.6(3.2)b	3.5(0.0)a	3.9(0.2)a
E. punctata	5.0(0.1)b	115(8.4)b	23(1.3)a	0.27(0.01)a	0.7(0.01)ab	80.3(4.9)ab	3.6(0.1)a	3.9(0.2)a
D.clandestineum[*]	1.7(0.1)c	151(7.1)a	93(3.7)b	0.71(0.06)c	1.1(0.02)c	159.7(11.5)c	2.9(0.2)b	4.2(0.2)a
P. coloratum	5.1(0.1)a	105(7.0)ab	21(1.2)a	0.36(0.02)a	0.7(0.01)a	73.9(4.8)ab	4.3(0.1)a	3.7(0.2)a
P. milicea	4.9(0.1)a	134(8.9)a	27(1.3)a	0.33(0.01)a	0.7(0.01)a	85.7(5.6)ac	3.9(0.1)b	2.6(0.1)b
P. queenslandicum	5.0(0.1)a	86(9.1)b	17(1.6)a	0.24(0.02)b	0.7(0.03)a	59.0(4.7)b	3.9(0.0)b	2.3(0.1)b
P. white	4.8(0.1)a	115(7.7)ab	23(1.1)a	0.30(0.02)ab	0.7(0.01)a	77.6(4.7)ab	4.1(0.0)ab	2.2(0.3)b
P. bisulcatum[*]	1.6(0.1)b	93(7.0)b	64(4.4)b	0.47(0.01)c	1.1(0.04)b	100.1(4.3)c	3.2(0.0)c	4.9(0.3)c
A. pur. Var. long	5.3(0.1)a	100(8.3)a	19(1.2)a	0.35(0.02)a	0.8(0.02)ab	118.7(8.8)a	4.9(0.1)a	2.5(0.2)a
S. obtusa	5.8(0.1)b	158(10.0)b	28(1.7)b	NA	0.7(0.02)a	82.0(5.9)b	NA	2.6(0.0)a
S. ciliata	5.4(0.1)ab	146(9.6)b	26(1.5)b	0.34(0.02)a	0.8(0.02)b	117.3(8.0)a	4.7(0.1)a	2.9(0.0)a
E. obstusa	5.8(0.1)a	191(13.3)a	33(2.1)a	0.46(0.04)a	0.8(0.02)a	138.6(6.2)a	4.1(0.0)a	2.6(0.2)a
F. africana	5.4(0.1)a	145(8.4)b	27(1.4)ab	0.52(0.02)a	0.7(0.02)a	108.0(3.2)b	3.9(0.1)a	2.5(0.2)a
S. fimbriatus	5.0(0.2)b	105(8.3)c	21(1.3)b	0.28(0.01)b	0.6(0.01)a	67.4(5.3)c	3.9(0.1)a	2.9(0.1)a
C. sp.[*]	1.6(0.1)c	96(5.7)c	63(4.9)c	0.61(0.07)a	1.2(0.05)b	114.8(2.7)b	3.0(0.2)b	2.7(0.2)a
E. obtusa	5.3(0.1)a	127(12.7)a	23(1.9)a	0.30(0.02)a	0.7(0.02)a	92.5(6.4)a	4.7(0.2)a	NA
M. caerulea[*]	1.9(0.1)b	61(3.7)b	32(3.1)b	0.32(0.02)a	1.0(0.04)b	57.7(3.3)b	3.6(0.1)b	3.6(0.2)
E. frumentacea	5.2(0.1)	85(7.2)	17(1.0)	0.26(0.03)	0.61(0.02)	49.2(3.0)	4.0(0.0)	4.1(0.2)

Table 2 Phylogenetic results of the best-fitted models and their parameters for photosynthesis parameters (summarizing Table S2-S10). If the values for C_3 and C_4 were different, it meant there were significant different values for C_3 and C_4 species (the evolutionary model with two different values of the root fit significantly better than the evolutionary model with the similar root).

Property	Model	AICw	Root

		Model type		C_3	C_4
J_{max}/V_{cmax}	Model 5	OU	1.000	1.59	5.15
V_{cmax}	Model 5	OU	0.902	59.46	23.03
J_{max}	Model 5	OU	0.620	88.72	124.88
Total Chl	Model 1	BM	0.409	0.36	
ETR/J_{max}	Model 5	OU	1.000	1.08	0.68
Chl a/b	Model 5	OU	0.995	3.40	4.61
ETR	Model 1	BM	0.465	88.94	
V_{pmax}	Model 4	OU	0.954	46.55	
V_{pmax}/V_{cmax}	Model 4	OU	0.977	1.97	
N	Model 5	OU	0.617	3.62	2.53

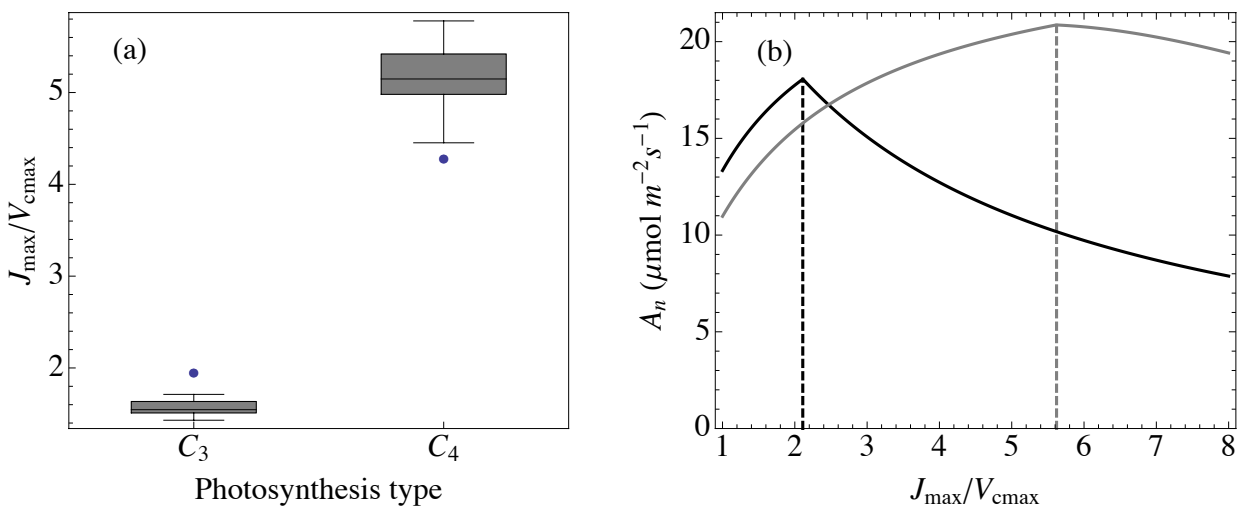

Fig. 1 Empirical measurements (a) and optimal modeling results (b) of J_{max}/V_{cmax} for C_3 and C_4 under ψ_S=-0.5 MPa, VPD=0.625, temperature of 25 °C and light intensity of 2000 μmol m^{-2} s^{-1}, the approximate greenhouse growth conditions. In (b), the black line represents C_3 and grey line represents C_4.

Higher J_{max}/V_{cmax} in C_4 is mainly driven by lower V_{cmax}

We looked further into how such a higher J_{max}/V_{cmax} in C_4 species is reached by comparing other empirical measurements. We found that although in some C_4 species J_{max} is higher, a lot of C_4 species did not have significantly higher J_{max} than their closely-related C_3 species, and measurements of total chlorophyll content were also similar (Table 1). However, our phylogenetic analysis detected a significant higher root state for J_{max} in C_4 than in C_3 (Table 2).

Conversely, V_{cmax} is significantly lower in nearly all C_4 species than in the closely-related C_3 species and phylogenetic analysis confirmed a higher V_{cmax} in C_3 (Table 1, 2). In order to look at the potential effects of decreasing V_{cmax} on assimilation rate, we held the J_{max} as constant and changed the V_{cmax} from 100% to 50% of the original C_3 parameter values in the C_3 and C_4 models. A decrease in V_{cmax} will significantly decrease the assimilation rates of C_3 species from 10 °C to 35°C, while decreasing V_{cmax} has little effects on the assimilation rates of C_4 species (Fig. 2). V_{cmax}, J_{max}, and chlorophyll also did not show significant differences among subtypes (Table S3-5, S12-14).

Variation in optimal J_{max}/V_{cmax} with environmental conditions

To understand how the J_{max}/V_{cmax} is predicted to vary across environmental gradients (Fig. 3), we calculated its optimal value for different CO_2 concentration, water limitation, and light intensities. The optimal J_{max}/V_{cmax} is predicted to increase linearly in both C_3 and C_4 species with increasing CO_2 concentration, but more steeply in C_3 species (Fig. 3a). The optimal J_{max}/V_{cmax} decreases similarly in both C_3 and C_4 species along with increasing water limitation (Fig. 3a). The optimal J_{max}/V_{cmax} is predicted to increase in both C_3 and C_4 species with decreasing light intensity and increasing temperatures (Fig. 3b). The changes of J_{max}/V_{cmax} with water limitation, light intensity, and temperature are non-linear, with the rate-of-change increasing greatly after a threshold (water limitation of ψ_S=-1, VPD=1.25, the light intensity of 800 μmol m^{-2} s^{-1} and temperature of 30 °C).

The ETR, calculated from fluorescence measurements, to J_{max} ratio was significantly higher ratio in C_3 species than that in their closely related C_4 species, with averages of 106% and 67.8% for C_3 and C_4 respectively (Table 1). Phylogenetic analysis indicated the root state of ETR itself is higher in C_4 species, but the differences are not significant (Table 2). Chlorophyll a/b is significantly higher in C_4 species than C_3 species, which is confirmed by both comparing closely-related C_4 and C_3 species within clusters (Fig 5c) and phylogenetic analysis (Table 2). Phylogenetic analysis indicates only Chlorophyll a/b is significantly different among subtypes (Table S7, S16). We also modeled the effects of O_2 accumulation on the C_4 assimilation rate, and there was very little change in assimilation when α ranged from 0 to 1 (Fig. S1). The value α indicates a change in the proportion of O_2 evolution in the bundle sheath where α=1 represents all O_2 evolution emanating from electron transport occurring in the bundle sheath and α=0 represent zero O_2 accumulation.

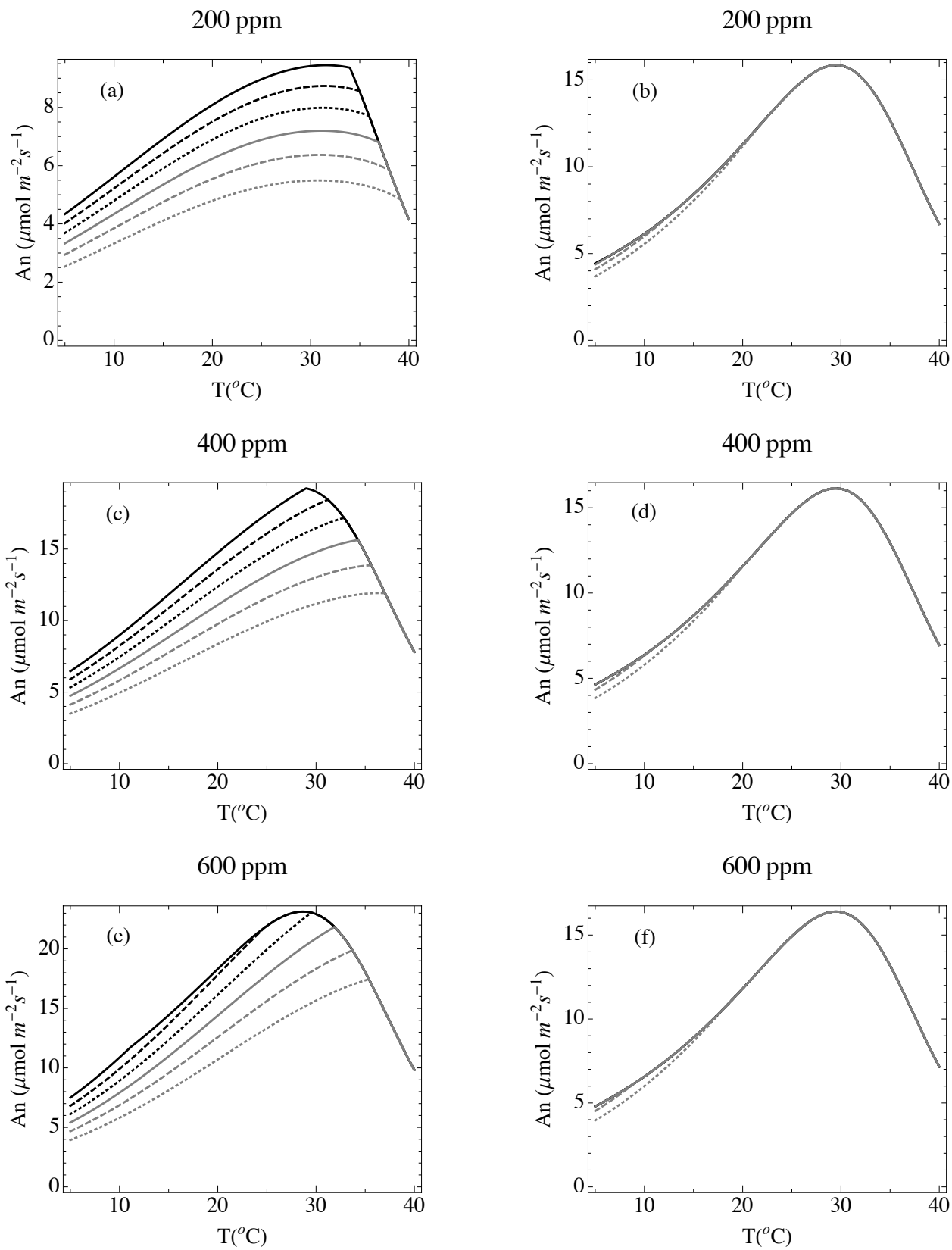
200 ppm
(a)
200 ppm
(b)
400 ppm
(c)
400 ppm
(d)
600 ppm
(e)
600 ppm
(f)
An (μmol $m^{-2}s^{-1}$)
T(^{o}C)

Fig. 2 Modeling results of changing V_{cmax} on assimilation rates (A_n) for C_3 (acd) and for C_4 (bdf) under different CO_2. Solid black line: the initial modeling condition of V_{cmax} (a typical C_3 value of 69 μmol m^{-2} s^{-1}); dashed black line: 90% of the initial V_{cmax}; dotted black line: 80% of the initial V_{cmax}; solid grey line: 70% of the initial V_{cmax}; dashed grey line: 60% of the initial V_{cmax}; dotted grey line: 50% of the initial V_{cmax}. C_3 and C_4 shared similar parameters except for the carbon concentration mechanism and different hydraulic conductance to mimic the initial origin of C_4 (full model and other parameters are shown in Zhou et al. (2018)).

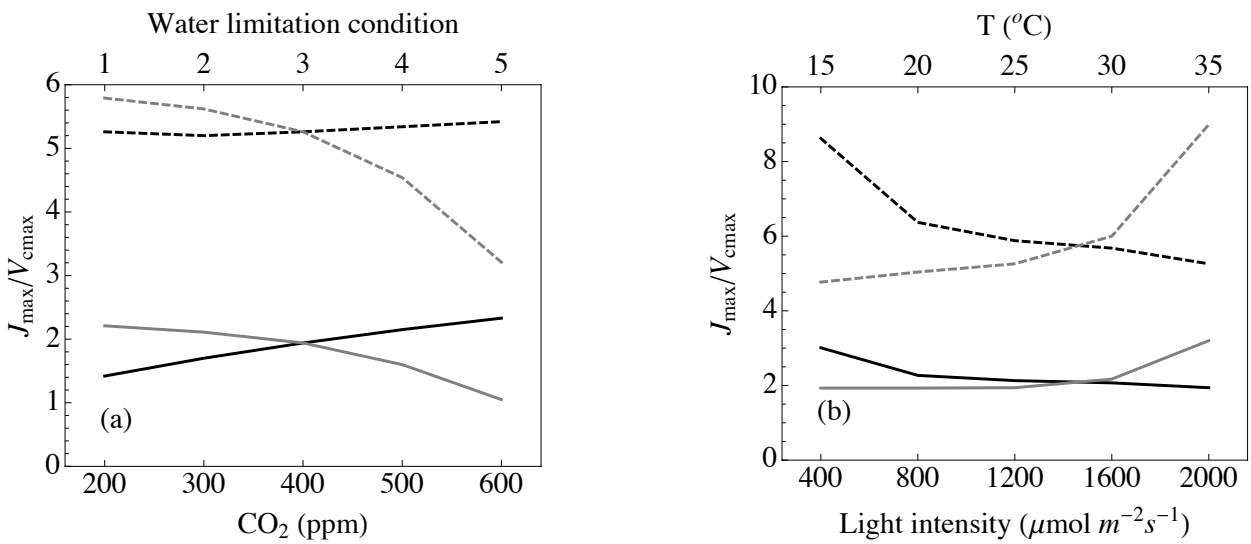

Fig. 3 Modeling results of optimal J_{max}/V_{cmax} for C_3 (solid lines) and C_4 (dashed lines) under different environmental conditions. (a) Black lines depict different CO_2 concentrations (bottom axis); grey lines different water limitation conditions (top axis; 1: saturated water; 2: ψ_S=-0.5 MPa, VPD=0.625; 3: ψ_S=-1 MPa, VPD=1.25; 4: ψ_S=-1.5 MPa, VPD=1.875; 5: ψ_S=-2 MPa, VPD=2.5). (b) Black lines depict optimal J_{max}/V_{cmax} different light intensities (bottom axis); grey lines for different temperatures (top axis). C_3 and C_4 parameters shared similar parameters except for the carbon concentration mechanism and different hydraulic conductance to mimic the initial origin of C_4 and most-closely related C_3 and C_4 species.

The empirical measurements and phylogenetic analysis indicate V_{pmax}/V_{cmax} are under the stabilized selection for a stabilized optimum of 1.97 and a range from 1.35 to 2.47, although

there is a variation of V_{pmax} (Fig. 4, Table 2). Again, no evidence shows there are differences among subtypes (Table S9-10, S18-19). The empirical values are higher than the optimal modeling result of V_{pmax}/V_{cmax} under 400 ppm, but similar to optimal modeling V_{pmax}/V_{cmax} under a CO_2 concentration of 200-300 ppm (Fig. 5). If we looked at the effects of V_{pmax}/V_{cmax} on the assimilation rate, the assimilation rate increase significantly with the increase of V_{pmax}/V_{cmax} from 0.5 to 1, but only decrease a little bit with a further increase of V_{pmax}/V_{cmax} (Fig. 5). We also modeled the V_{pmax}/V_{cmax} under different environmental conditions. V_{pmax}/V_{cmax} decreases along with the increase of the CO_2 concentration, especially when CO_2 decrease from 200 ppm to 300 ppm, but the change is little when CO_2 is above 400 ppm (Fig. S2a). V_{pmax}/V_{cmax} increases along with the increase of water limitation condition and relatively decrease with the rise in temperature (Fig. S2a, b). The optimal V_{pmax}/V_{cmax} decreases with the change of light intensity (Fig. S2b).

Fig. 4 Bar plot for the photosynthetic parameters of V_{pmax} and V_{pmax}/V_{cmax} for C_4 species. Each cluster indicates the most closely related C_4 species. Letters above bars indicates whether there are significant differences for the species within each cluster. Error bars indicate standard errors.

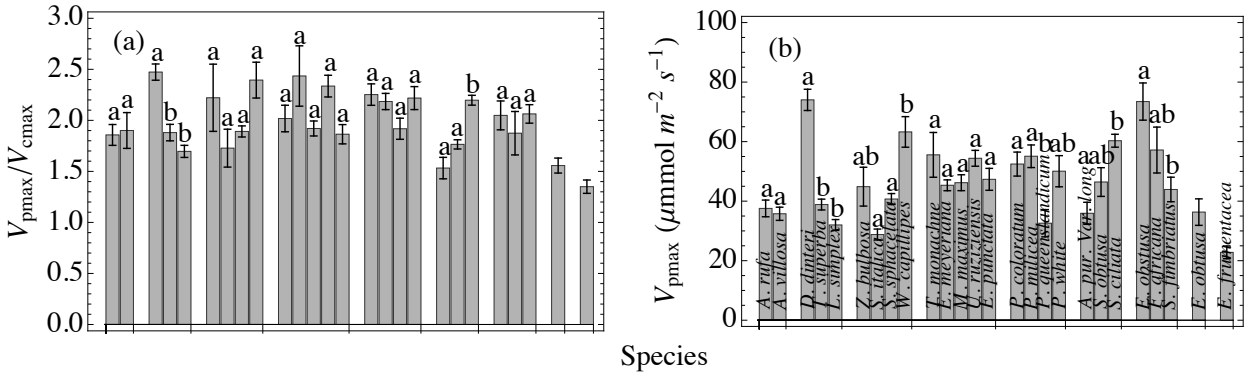

Fig. 5 Modeling results of assimilation rate with varying V_{pmax}/V_{cmax} under different CO_2 concentration and ψ_S=-1MPa, VPD=1.25, temperature of 25 °C and light intensity of 2000 μmol m^{-2} s^{-1}.

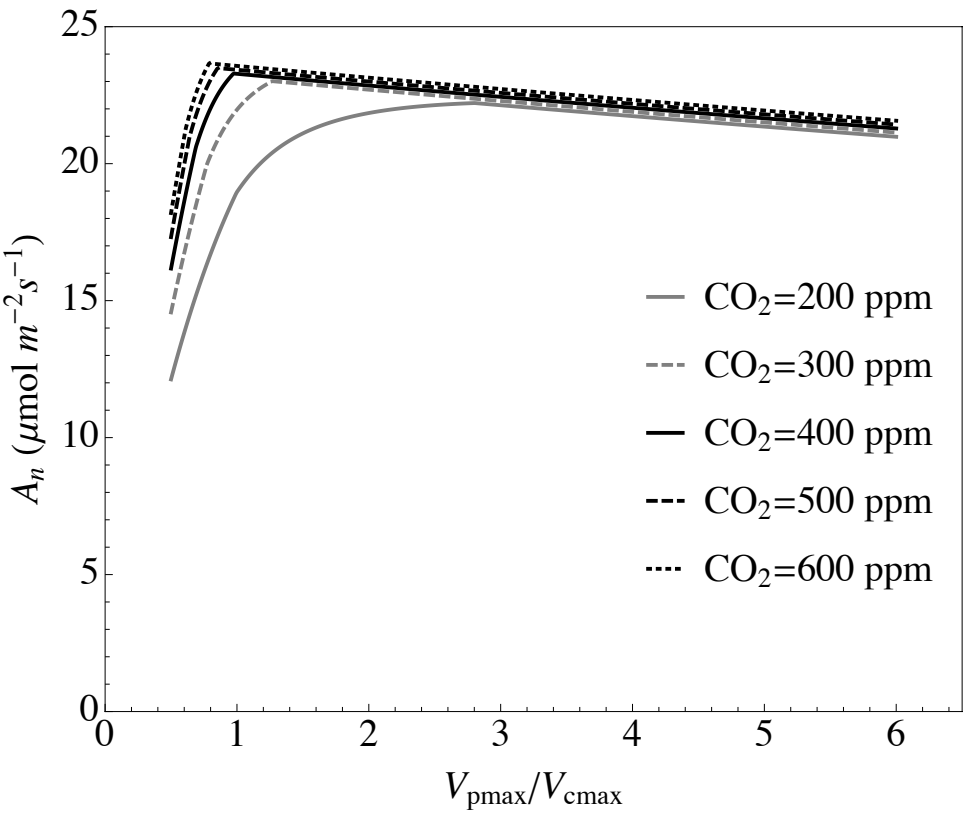

Since there is a great variation of total nitrogen content in the plants and there is uncertainty in the stoichiometry of PEPC, we performed sensitivity analysis for the optimal modeling of J_{max}/V_{cmax} and V_{pmax}/V_{cmax}. For C_3 photosynthesis, optimal J_{max}/V_{cmax} increases slightly with decreasing total nitrogen (7.73% increase of J_{max}/V_{cmax} with 50% reduction in total nitrogen), while for C_4, optimal J_{max}/V_{cmax} decreases with total nitrogen (20.34% increase of J_{max}/V_{cmax} with 50% reduction in total nitrogen) (Fig. S3a). The optimal V_{pmax}/V_{cmax} increases somewhat with decreasing total nitrogen (15.3% increase of V_{pmax}/V_{cmax} with 50% reduction in total nitrogen) (Fig. S3a). The optimal J_{max}/V_{cmax} is relatively constant with the change of stoichiometry of PEPC from 50% to 200%, but increases as the stoichiometry increases from 200% to 800% (Fig. S3b). Also, the optimal V_{pmax}/V_{cmax} is relatively constant with the variation of the $1/(6.72\times V_{pr} \times \xi)$ term.

Discussion

The evolution of C_4 photosynthesis was likely associated with several important shifts in photosynthetic traits. Our results show that one of these shifts was the allocation of nitrogen resources between the CB cycle and the light reactions, resulting in a higher J_{max}/V_{cmax} for C_4

than C_3 species. An increase in J_{max}/V_{cmax} due to reallocation of nitrogen is likely a crucial evolutionary step for C_4 evolution after the CCM evolved, and it is important to look at how it may have occurred. Zhou et al. (2018) proposed that if nitrogen is reallocated from the CB cycle (e.g., Rubsico) to the light reactions (an increase in J_{max}, and a decrease in V_{cmax}), the assimilation rate of C_4 would significantly increase because the extra ATP costs could be satisfied, and within the CCM Rubisco operates more efficiently, which means less of the enzyme is required. Our optimality model confirms this intuition, predicting higher J_{max}/V_{cmax} for C_4 species than C_3. Our empirical measurements conform to this prediction qualitatively. All C_4 grasses have a lower V_{cmax} than the closely-related C_3 in the current study, which suggests C_4 photosynthesis does allow for less investment of nitrogen in Rubisco.

Previous empirical measurements of J_{max}/V_{cmax} from previous studies reported greater variation than we found in our measurements and a range from 2 to 6 for C_4 species (Massad et al., 2007; Ye et al., 2013; Ge et al., 2014; Bellasio et al. 2016), although the average across these studies is close to our measurement of 5.1. The variation may result from the uncertainty of previous estimation methods for C_4 photosynthesis, uncertainties that we have assuaged with our work. Previous modeling work assumed a high J_{max}/V_{cmax} for C_4, while considering similar nitrogen content in C_3 and C_4 (Vico and Porporato, 2008; Osborn and Sack, 2012). Our results validate these assumptions based on new empirical data and optimality modeling.

Similar results were either proposed or found by Brown (1978), Ku et al. (1979), Sage et al. (1987) and Sharwood et al. (2016). Tissue et al. (1995) and Ghannoum et al. (2010) detected lower Rubisco content and higher chlorophyll and thylakoid content, supporting reallocation within the leaf. Any surplus nitrogen could be distributed among three broad categories: 1) reallocated to the light reactions or 2) stored or used to construct new organs or 3) simply not taken up, thus reducing plant nitrogen requirements. Our empirical measurements provide evidence for all of these options, although we cannot differentiate between the second and third. Some of our C_4 species, e.g., *Danthoniopsis dinteri* and *Panicum milicea*, had a significantly higher J_{max} than closely-related C_3 which suggests nitrogen reallocation from the CB cycle to the light reactions. Phylogenetic analysis results also supports such a reallocation happened generally with a significant higher J_{max} in C_4. Several C_4 grasses we measured, however, had a J_{max} that was similar to closely related C_3 species, while maintaining a lower V_{cmax}. Our modeling

results show that decreasing V_{cmax} by 50% has little effect on the assimilation rate. ANOVA tests showed that both hypothesis 2) and 3) could happened together with hypothesis 1), because some C_4 species have significant lower nitrogen content, but some have equivalent values. However, phylogenetic analysis of nitrogen indicated that in general, C_4 species have a lower nitrogen content than C_3 species, which support option 3). It is worth considering the potential ecological and evolutionary ramifications. Firstly, in a nitrogen-depleted habitat, C_4 could have a competitive advantage as confirmed by Riley et al. (2008; although Sage and Pearcy, 1987, found no evidence for this). In habitats where nitrogen is not limiting, the excess nitrogen could be used to construct more leaf area (Sage and Pearcy, 1987; Anten et al., 1995; Riley et al., 2008), and greater leaf area in the early stages of growth was indeed seen by Atkinson et al. (2016). On the other hand, the lack of nitrogen reallocation from the CB cycle to the light reactions may indicate physiological constraints in fertile habitats. For example, photorespiration in C_3 plants is proposed to enhance the nitrate metabolism (Oaks, 1994; Rachmilevitch et al., 2004; Bauwe et al., 2010; Bloom, 2015), therefore the formation of CCM, which inhibits photorespiration, may reduce overall plant-available nitrogen for C_4 species.

The extra ATP required to run the C_4 CCM is generated primarily by cyclic electron transport, and this likely evolved to balance ATP:NADPH stoichiometry, as opposed to minimizing O_2 production. Aside from cyclic electron transport, all mechanisms that provide extra ATP are associated with the O_2-producing PSII (Kramer and Evans, 2011), and would not lead to a significant increase of chl a/b as found here and in other studies (Ku et al., 1991). However, chl a/b differ among subtypes may indicate there could be different types or different magnitudes of electron transport pathways to support the CCM in different subtypes. Our model results show that a wide-range of O_2 concentration in the bundle sheath has minimal impact on photosynthetic rate, and therefore indicate that decreasing O_2 evolution is not the driving force behind increasing cyclic electron transport. Rather, our results support the alternative hypothesis cyclic electron transport balances the stoichiometry of NADPH and ATP demand (Nakamura et al., 2013; Ishikawa et al., 2016; Munekage and Taniguchi, 2016). The ETR/J_{max} indicated a relatively consistent proportion of PSII fluorescence to total electron transport across all C_4 species, which did not significantly different among C_4 subtypes. The reason could be that although the stoichiometry of NADPH and ATP is different between mesophyll cells and bundle

sheath cells in NADP-ME and NAD-ME subtypes, the total stoichiometry is the same (Hatch et al., 1987; Kanai and Edwards, 1999; Takabayashi et al., 2005; Yin et al., 2018).

In C_3 species, the fluorescence-based ETR is widely used as an approximation of J_{max} (Baker *et al.* 2007; Sage and Kubien, 2007; Yin et al., 2009); however, the estimation method has not previously been suitable to C_4 pathway because the fluorescence-based ETR does not account for the contribution of cyclic-electron transport to J_{max}. Because we found a relatively constant ETR/J_{max} for all C_4 species, we can assume a constant proportion of electron cycling and thus, we can now expand approaches that use combined gas exchange and fluorescence to estimate the J_{max} as well as other C_4 photosynthetic parameters. Yin et al. (2011) use an assumed value of 60% for ETR/J_{max}, which assumed that all electron transport for PEP regeneration was not from linear electron transport, which is a little lower than our value of 67.8%. The theoretical modeling analysis of Yin and Struik (2012) and Yin and Struik (2018) predicted cyclic electron transport could account for 45% or 50% of total J_{max}.

The tight coordination between RuBP carboxylation and PEP carboxylation likely occurred early in the evolution of the C_4 of CCM, leading to a relatively constant V_{pmax}/V_{cmax}. There were few V_{pmax}/V_{cmax} values reported in previous studies, but our results are comparable with existing ones. Yin et al. (2011) and Yin et al., (2016) reported estimation results of 2.43 and 2.5 respectively for V_{pmax}/V_{cmax}. Estimates from biochemical measurements of Pengelly et al. (2010) and Kubien et al. (2003) were 2.1-2.5 and 3.1 respectively. Our empirical V_{pmax}/V_{cmax} is in line with the optimal modeling results under 200-300 ppm, as opposed to CO_2 concentrations closer to current growth conditions. All extant C_4 species have gone through a low CO_2 bottleneck over the last 5 million years. It is possible that this bottleneck represented strong selection to increase the V_{pmax}/V_{cmax} to maintain a high assimilation rate. As CO_2 has risen, V_{pmax}/V_{cmax} has exceeded the optimal V_{pmax}/V_{cmax}, but the effects of a high V_{pmax}/V_{cmax} on assimilation rate at elevated CO_2 were minimal.

Our improved estimates of J_{max}/V_{cmax} and V_{pmax}/V_{cmax} for C_4 plants can aid predictions of net primary productivity by large-scale models. J_{max}/V_{cmax} is an important input parameter in biogeochemical cycle, biodiversity or productivity models (e.g., Biome-BGC, Community Land Model) (Beerling and Quick, 1995; Zaehle et al., 2005; Bonan et al., 2011; Walker et al., 2014),

however, there have been no reliable parameters reported for C_4 species. Our results suggests a value of around 5 supported both optimality modeling and empirical measurements. Our optimality modeling framework can also be used to adaptive plasticity (or acclimation) of J_{max}/V_{cmax} under different environmental conditions that can be used to predict responses of ecosystems to future climate change. Previous modeling (Sage, 1990; Hikosaka and Terashima, 1995) and experimental studies (Evans, 1989b; Pons and Pearcy, 1994; Tissue, 1999; Onoda et al., 2005) indicated higher allocation to the light reactions (namely, higher J_{max}/V_{cmax}) under shade, elevated CO_2 and higher temperature for C_3 species, which is consistent with our predictions. However, C_3 and C_4 species could respond differently to environmental variation (Ward et al., 1999; Wand et al., 1999; Ripley et al., 2013), and our modeling suggests that the acclimation to CO_2 in C_4 species may be of a lesser extent than C_3 species (Sage and McKown, 2005. Additionally, V_{pmax}/V_{cmax} may be a legacy of ancient environmental conditions, and its plasticity may be lower, but this requires further examination. Generally, not all species or physiological traits may be plastic along with environmental change (Herrick and Thomas, 2001; Kubiske et al., 2002); therefore, further exploring acclimation and genetic constraints will be important for predicting species responses to climate change.

In conclusion, here we examined the divergence of photosynthetic traits between C_3 and C_4 grasses after the evolution of the C_4 CCM. Our results contribute to our understanding of the ecological and evolutionary consequences of this important evolutionary innovation. Unlike the divergence and reorganization of hydraulic traits, which may follow an evolutionary trend (Zhou, 2020), we find that photosynthetic properties are under stabilizing selection. Such observations may indicate that photosynthetic properties were under much stronger selective pressures or evolved step by step along with the CCM, and once the CCM formed, photosynthetic properties quickly reach stable states, whereas hydraulic properties responded after the formation the CCM and the selective pressure was lower.

Acknowledgements

H. Z. and this research is supported by the NOAA Climate and Global Change Postdoctoral Fellowship Program, administered by UCAR's Cooperative Programs for the Advancement of Earth System Science (CPAESS) under award #NA18NWS4620043B and is also supported by the Dissertation Completion Fellowship provided by the Graduate Division of School of Arts and

Sciences, University of Pennsylvania. B.R.H is supported by NSF-IOS award 1856587. We sincerely thank Dr. Matteo Detto (Princeton University) for his help in building the optimal models for J_{max}/V_{cmax}.

Author Contribution

HZ, EA, and BH conceptualized the idea. HZ and BH designed the experiments and methods. HZ and EA built the optimal models. HZ performed the modeling work, performed empirical measurements and analyzed the data. HZ wrote the first draft, BH and EA contributed substantially to revisions.

Reference

Anten NP, Schieving F, Medina E, Werger MJA, Schuffelen P (1995) Optimal leaf area indices in C_3 and C_4 mono-and dicotyledonous species at low and high nitrogen availability. Physiologia plantarum 95(4): 541-550.

Aubry S, Brown NJ, Hibberd JM (2011) The role of proteins in C_3 plants prior to their recruitment into the C_4 pathway. Journal of experimental botany 62(9): 3049-3059.

Atkinson RR, Mockford EJ, Bennett C, Christin PA, Spriggs EL, Freckleton RP, Thompson K, Rees M, Osborne CP (2016) C_4 photosynthesis boosts growth by altering physiology, allocation and size. Nature Plants 2(5): 16038.

Baker NR, Harbinson J, Kramer DM (2007) Determining the limitations and regulation of photosynthetic energy transduction in leaves. Plant, Cell & Environment 30(9): 1107-1125.

Baker NR, Long SP (1988) Photosynthesis and temperature, with particular reference to effects on quantum yield. In Plants and Temperature: Society for Experimental Biology Symposium No. XXXXII. Company of Biologists (eds S.P. Long & F.I. Woodward), pp. 347–375. Company of Biologists, Cambridge, UK.

Bauwe H, Hagemann M, Fernie AR (2010) Photorespiration: players, partners and origin. Trends in plant science *15*(6): 330-336.

Beerling DJ, Quick WP (1995) A new technique for estimating rates of carboxylation and electron transport in leaves of C_3 plants for use in dynamic global vegetation models. Global Change Biology 1(4): 289-294.

Bellasio C, Beerling DJ, Griffiths H (2016) An Excel tool for deriving key photosynthetic parameters from combined gas exchange and chlorophyll fluorescence: theory and practice. Plant, cell & environment 39(6): 1180-1197.

Bellasio C, Burgess SJ, Griffiths H, Hibberd JM (2014) A high throughput gas exchange screen for determining rates of photorespiration or regulation of C_4 activity. J Exp Bot 65:3769-3779

Bloom AJ (2015) Photorespiration and nitrate assimilation: a major intersection between plant carbon and nitrogen. Photosynthesis Research 123(2): 117-128.

Bonan GB, Lawrence PJ, Oleson KW, Levis S, Jung M, Reichstein M, Lawrence DM, Swenson SC (2011) Improving canopy processes in the Community Land Model version 4 (CLM4) using global flux fields empirically inferred from FLUXNET data. Journal of Geophysical Research: Biogeosciences 116(G2).

Brown RH (1978) A difference in N use efficiency in C_3 and C_4 plants and its implications in adaptation and evolution 1. Crop Science 18(1): 93-98.

Brown RH, Byrd GT (1993) Estimation of bundle sheath cell conductance in C_4 species and O_2 insensitivity of photosynthesis. Plant Physiol 103:1183-1188.

von Caemmerer S (2000) *Biochemical models of photosynthesis. In Techniques in Plant Sciences*. CSIRO Publishing, Colingwood, Australia, pp 91–122.

von Caemmerer S, Furbank RT (2016) Strategies for improving C_4 photosynthesis. Current Opinion in Plant Biology 31: 125-134.

Cavender-Bares J, Kozak KH, Fine PV, Kembel SW (2009) The merging of community ecology and phylogenetic biology. Ecology letters 12(7): 693-715.

Christin PA, Osborne CP (2014) The evolutionary ecology of C_4 plants. New Phytologist *204*(4): 765-781.

Christin PA, Boxall SF, Gregory R, Edwards EJ, Hartwell J, Osborne CP (2013a) Parallel recruitments of multiple genes into C_4 photosynthesis. Genome Biology and Evolution 5: 2174–2187.

Christin PA, Osborne CP, Chatelet DS, Columbus JT, Besnard G, Hodkinson TR, Garrison LM, Vorontsova MS, Edwards EJ (2013b) Anatomical enablers and the evolution of C_4 photosynthesis in grasses. Proceedings of the National Academy of Sciences 110(4): 1381-1386.

Collatz GJ, Ribas-Carbo M, Berry JA (1992) Coupled photosynthesis-stomatal conductance model for leaves of C_4 plants. Functional Plant Biology 19(5): 519-538.

Croft H, Chen JM, Luo X, Bartlett P, Chen B, Staebler RM (2017) Leaf chlorophyll content as a proxy for leaf photosynthetic capacity. Global change biology 23(9): 3513-3524.

Edwards EJ, Osborne CP, Strömberg CAE, Smith SA, C_4 Grasses Consortium. 2010. The origins of C_4 grasslands: integrating evolutionary and ecosystem science. Science 328: 587–591.

Edwards EJ, Still CJ, Donoghue MJ (2007) The relevance of phylogeny to studies of global change. Trends in Ecology & Evolution 22(5): 243-249.

Ehleringer JR, Cerling TE, Helliker BR (1997) C_4 photosynthesis, atmospheric CO_2, and climate. Oecologia 112(3): 285-299.

Ehleringer JR, Monson RK (1993) Evolutionary and ecological aspects of photosynthesis pathway variation. Annu Rev Ecol Syst 24: 411-439.

Ehleringer JR, Sage RF, Flanagan LB, Pearcy RW (1991) Climate change and the evolution of C_4 photosynthesis. Trends in ecology & evolution *6*(3):95-99.

Evans J R (1989a) Partitioning of nitrogen between and within leaves grown under different irradiances, Australian J Plant Physiol: 16, 533–548, doi:10.1071/PP9890533.

Evans JR (1989b) Photosynthesis and nitrogen relationships in leaves of C_3 plants. Oecologia 78(1) 9-19.

Evans J, Poorter H (2001) Photosynthetic acclimation of plants to growth irradiance: the relative importance of specific leaf area and nitrogen partitioning in maximizing carbon gain. Plant, Cell & Environment 24(8): 755-767.

Farquhar GD, Von Caemmerer S,Berry JA (1980) A biochemical model of photosynthetic carbon dioxide assimilation in leaves of 3-carbon pathway species. *Planta* 149(1):78–90.

Fujita N, Miwa T, Ishijima S, Izui K, Katsuki H (1984) The primary structure of phosphoenolpyruvate carboxylase of Escherichia coli. Nucleotide sequence of the ppc gene and deduced amino acid sequence. The Journal of Biochemistry 95(4): 909-916.

Ge ZM, Zhang LQ, Yuan L, Zhang C (2014) Effects of salinity on temperature-dependent photosynthetic parameters of a native C_3 and a non-native C_4 marsh grass in the Yangtze Estuary, China. Photosynthetica 52(4):484–492.

Genty B, Briantais JM, Baker NR (1989) The relationship between the quantum yield of photosynthetic electron transport and quenching of chlorophyll fluorescence. Biochimica et Biophysica Acta (BBA)-General Subjects 990(1): 87-92.

Ghannoum O, Evans JR, von Caemmerer S (2010) Nitrogen and water use efficiency of C_4 plants. In: C_4 photosynthesis and related CO_2 concentrating mechanisms (eds. Raghavendra, A.S. & Sage, R.F.). Springer Science, The Netherlands, Dordrecht, pp. 129–146.

Grass Phylogeny Working Group II (2012) New grass phylogeny resolves deep evolutionary relationships and discovers C_4 origins. New Phytol. 193, 304-312.

Griffiths H, Weller G, Toy LF, Dennis RJ (2013) You're so vein: bundle sheath physiology, phylogeny and evolution in C_3 and C_4 plants. Plant, Cell & Environment 36(2): 249-261.

Hatch MD (1987) C_4 photosynthesis: a unique blend of modified biochemistry, anatomy and ultrastructure. Biochim Biophys Acta 895(2):81-106.

Hatch MD, Osmond CB (1976) Compartmentation and transport in C_4 photosynthesis. In Transport in plants III (pp. 144-184). Springer, Berlin, Heidelberg.

Herrick JD, Thomas RB (2001) No photosynthetic down-regulation in sweetgum trees (Liquidambar styraciflua L.) after three years of CO_2 enrichment at the Duke Forest FACE experiment. Plant, Cell & Environment 24(1): 53-64.

Hikosaka K, Terashima I (1995) A model of the acclimation of photosynthesis in the leaves of C_3 plants to sun and shade with respect to nitrogen use. Plant, Cell & Environment 18(6), pp.605-618.

Ishikawa N, Takabayashi A, Sato F, Endo T (2016) Accumulation of the components of cyclic electron flow around photosystem I in C_4 plants, with respect to the requirements for ATP. Photosynthesis research 129(3): 261-277.

Kanai R, Edwards GE (1999) The biochemistry of C_4 photosynthesis. C_4 plant biology 49: p.87.

Kellogg EA (1999) Phylogenetics aspects of the evolution of C_4 photosynthesis. In: Sage RF, Monson RK, eds. C_4 plant biology. San Diego, CA, USA: Academic Press, 411–444.

Kramer DM, Evans JR (2011) The importance of energy balance in improving photosynthetic productivity. Plant Physiology 155(1): 70-78.

Kromdijk J, Long SP (2016) One crop breeding cycle from starvation? How engineering crop photosynthesis for rising CO_2 and temperature could be one important route to alleviation. Proceedings of the Royal Society B: Biological Sciences *283*(1826), p.20152578.

Kromdijk J, Ubierna N, Cousins AB, Griffiths H (2014) Bundle-sheath leakiness in C_4 photosynthesis: a careful balancing act between CO_2 concentration and assimilation. J Exp Bot 65:3443-3457

Ku MSB, Schmitt MR, Edwards GE (1979) Quantitative determination of RuBP carboxylase-orygenase protein in leaves of several C_3 and C_4 plants. *J Exp Bot* 114(1)89–98.

Kubien DS, von Caemmerer S, Furbank RT, Sage RF (2003) C_4 photosynthesis at low temperature. A study using transgenic plants with reduced amounts of Rubisco. Plant Physiology 132(3): 1577-1585.

Ku MS, Wu J, Dai Z, Scott RA, Chu C, Edwards GE (1991) Photosynthetic and photorespiratory characteristics of *Flaveria* species. Plant Physiology 96(2): 518-528.

Kubiske ME, Zak DR, Pregitzer KS, Takeuchi Y (2002) Photosynthetic acclimation of overstory Populus tremuloides and understory Acer saccharum to elevated atmospheric CO_2 concentration: interactions with shade and soil nitrogen. Tree Physiology 22(5): 321-329.

Lundgren MR, Dunning LT, Olofsson JK, MorenoVillena JJ, Bouvier JW, Sage TL, Khoshravesh R, Sultmanis S, Stata M, Ripley BS, Vorontsova MS (2019) C_4 anatomy can evolve via a single developmental change. Ecology letters 22(2): 302-312.

Mallmann J, Heckmann D, Bräutigam A, Lercher MJ, Weber AP, Westhoff P, Gowik U (2014) The role of photorespiration during the evolution of C_4 photosynthesis in the genus Flaveria. *Elife 3*:p.e02478.

Massad RS, Tuzet A, Bethenod O (2007) The effect of temperature on C_4-type leaf photosynthesis parameters. Plant Cell Environ 30(9):1191-1204.

McKown AD, Dengler NG. 2007. Key innovations in the evolution of Kranz anatomy and C_4 vein pattern in Flaveria (Asteraceae). American Journal of Botany 94: 382–399.

Munekage YN (2016) Light harvesting and chloroplast electron transport in NADP-malic enzyme type C_4 plants. Current opinion in plant biology 31: 9-15.

Munekage YN, Taniguchi YY (2016) Promotion of cyclic electron transport around photosystem I with the development of C_4 photosynthesis. Plant and Cell Physiology 57(5): 897-903.

Nakamura N, Iwano M, Havaux M, Yokota A, Munekage YN (2013) Promotion of cyclic electron transport around photosystem I during the evolution of NADP–malic enzyme-type C_4 photosynthesis in the genus *Flaveria*. New Phytologist 199(3): 832-842.

Niinemets Ü, Tenhunen JD (1997) A model separating leaf structural and physiological effects on carbon gain along light gradients for the shade-tolerant species *Acer saccharum*. Plant Cell Environ 20(7): 845–866, doi:10.1046/j.1365-3040.1997.d01-133.x.

Oaks A (1994) Efficiency of nitrogen utilization in C_3 and C_4 cereals. Plant Physiology 106(2): p.407.

Ögren E and Evans JR (1993) Photosynthetic light response curves.1. The influence of CO_2 partial pressure and leaf inversion. Planta 189(2):182-190.

Onoda Y, Hikosaka K, Hirose T (2005) The balance between RuBP carboxylation and RuBP regeneration: a mechanism underlying the interspecific variation in acclimation of photosynthesis to seasonal change in temperature. Functional Plant Biology 32(10): 903-910.

Osborne CP, Sack L (2012) Evolution of C_4 plants: a new hypothesis for an interaction of CO_2 and water relations mediated by plant hydraulics. Philosophical Transactions of the Royal Society B: Biological Sciences 367(1588): 583-600.

Pengelly JJ, Sirault XR, Tazoe Y, Evans JR, Furbank RT, von Caemmerer S (2010) Growth of the C_4 dicot Flaveria bidentis: photosynthetic acclimation to low light through shifts in leaf anatomy and biochemistry. Journal of experimental botany 61(14): 4109-4122.

Pearcy RW, Ehleringer J (1984) Comparative ecophysiology of C_3 and C_4 plants. Plant, Cell & Environment 7(1): 1-13.

Pons TL, Pearcy RW (1994) Nitrogen reallocation and photosynthetic acclimation in response to partial shading in soybean plants. Physiologia Plantarum 92(4): 636-644.

Porra RJ, Thompson WA, Kriedemann PE (1989) Determination of accurate extinction coefficients and simultaneous equations for assaying chlorophylls a and b extracted with four different solvents: verification of the concentration of chlorophyll standards by atomic absorption spectroscopy. Biochimica et Biophysica Acta (BBA)-Bioenergetics 975(3): pp.384-394.

Quebbeman JA, Ramirez JA (2016) Optimal allocation of leaf-level nitrogen: Implications for covariation of Vcmax and Jmax and photosynthetic downregulation. Journal of Geophysical Research: Biogeosciences 121(9): 2464-2475.

Rachmilevitch S, Cousins AB, Bloom AJ (2004) Nitrate assimilation in plant shoots depends on photorespiration. Proceedings of the National Academy of Sciences 101(31): 11506-11510.

Raines CA (2011) Increasing photosynthetic carbon assimilation in C_3 plants to improve crop yield: current and future strategies. Plant physiology 155(1): 36-42.

Ripley BS, Abraham TI, Osborne CP (2008) Consequences of C_4 photosynthesis for the partitioning of growth: a test using C_3 and C_4 subspecies of *Alloteropsis semialata* under nitrogen-limitation. Journal of experimental botany 59(7): 1705-1714.

Ripley BS, Cunniff J, Osborne CP (2013) Photosynthetic acclimation and resource use by the C_3 and C_4 subspecies of *Alloteropsis semialata* in low CO_2 atmospheres. Global Change Biology 19(3): 900-910.

Rodriguez-Calcerrada J, Reich PB, Rosenqvist E, Pardos JA, Cano FJ, Aranda I (2008) Leaf physiological versus morphological acclimation to high-light exposure at different stages of foliar development in oak. Tree physiology 28(5): 761-771.

Sage RF (1990) A model describing the regulation of ribulose-1, 5-bisphosphate carboxylase, electron transport, and triose phosphate use in response to light intensity and CO_2 in C_3 plants. Plant Physiology *94*(4): 1728-1734.

Sage RF (2001) Environmental and evolutionary preconditions for the origin and diversification of the C_4 photosynthetic syndrome. Plant Biology 3: 202–213.

Sage RF (2004) The evolution of C_4 photosynthesis. New Phytologist 161: 341–370.

Sage RF (2016) Tracking the evolutionary rise of C_4 metabolism. Journal of experimental botany 67(10): 2919-2922.

Sage RF, Christin PA, Edwards EJ (2011) The C_4 plant lineages of planet Earth. Journal of experimental botany 62(9): 3155-3169.

Sage RF, Kubien DS (2007) The temperature response of C_3 and C_4 photosynthesis. Plant, cell & environment 30(9): 1086-1106.

Sage RF, McKown AD (2005) Is C_4 photosynthesis less phenotypically plastic than C_3 photosynthesis? Journal of experimental botany 57(2): 303-317.

Sage RF and Monson R, 1999. The taxonomic distribution of C_4 photosynthesis. C_4 plant biology. San Diego: Academic. P551-585.

Sage RF, Monson RK, Ehleringer JR, Adachi S, Pearcy RW (2018) Some like it hot: the physiological ecology of C4 plant evolution. Oecologia 187(4): 941-966.

Sage RF, Pearcy RW (1987) The nitrogen use efficiency of C_3 and C_4 plants: I. Leaf nitrogen, growth, and biomass partitioning in Chenopodium album (L.) and *Amaranthus retroflexus* (L.). Plant Physiology 84(3): 954-958.

Sage RF, Pearcy RW, Seemann JR (1987) The nitrogen use efficiency of C_3 and C_4 plants: III. Leaf nitrogen effects on the activity of carboxylating enzymes in *Chenopodium album* (L.) and *Amaranthus retroflexus* (L.). Plant physiology 85(2): 355-359.

Sage RF, Sage TL, Kocacinar F (2012) Photorespiration and the evolution of C_4 photosynthesis. Annual review of plant biology 63: 19-47.

Sharwood RE, Ghannoum O, Whitney SM (2016) Prospects for improving CO_2 fixation in C_3-crops through understanding C_4-Rubisco biogenesis and catalytic diversity. Current Opinion in Plant Biology 31: 135-142.

Still CJ, Berry JA, Collatz GJ, DeFries RS (2003) Global distribution of C_3 and C_4 vegetation: carbon cycle implications. Global Biogeochemical Cycles 17: 6.1–6.14.

Takabayashi A, Kishine M, Asada K, Endo T, Sato F (2005) Differential use of two cyclic electron flows around photosystem I for driving CO_2-concentration mechanism in C_4 photosynthesis. Proceedings of the National Academy of Sciences 102(46): 16898-16903.

Tissue DT, Griffin KL, Ball JT (1999) Photosynthetic adjustment in field-grown ponderosa pine trees after six years of exposure to elevated CO_2. Tree Physiology 19(4-5): 221-228.

Tissue DT, Griffin KL, Thomas RB, Strain BR (1995) Effects of low and elevated CO_2 on C_3 and C_4 annuals. II. Photosynthesis and leaf biochemistry. Oecologia 101(1):21-28.

Ubierna N, Sun W, Kramer DM, Cousins AB (2013) The efficiency of C_4 photosynthesis under low light conditions in *Zea mays*, *Miscanthus* X *giganteus* and *Flaveria bidentis*. Plant Cell Environ 36:365-381

Vicentini A, Barber JC, Aliscioni SS, Giussani LM, Kellogg EA (2008) The age of the grasses and clusters of origins of C_4 photosynthesis. Global Change Biology, 14(12): 2963-2977.

Vico G, Porporato A (2008) Modelling C_3 and C_4 photosynthesis under water-stressed conditions. Plant and Soil 313(1): 187-203.

Walker AP, Beckerman AP, Gu L, Kattge J, Cernusak LA, Domingues TF, Scales JC., Wohlfahrt G, Wullschleger SD, Woodward FI (2014) The relationship of leaf photosynthetic traits–V_{cmax} and J_{max}–to leaf nitrogen, leaf phosphorus, and specific leaf area: a meta-analysis and modeling study. Ecology and evolution 4(16): 3218-3235.

Walker BJ, Drewry DT, Slattery RA, VanLoocke A, Cho YB, Ort DR (2018) Chlorophyll can be reduced in crop canopies with little penalty to photosynthesis. Plant Physiology 176(2): 1215-1232.

Wand SJ, Midgley GF, Jones MH, Curtis PS (1999) Responses of wild C_4 and C_3 grass (Poaceae) species to elevated atmospheric CO_2 concentration: a meta-analytic test of current theories and perceptions. Global Change Biology 5(6): 723-741.

Ward JK, Tissue DT, Thomas RB, Strain BR (1999) Comparative responses of model C_3 and C_4 plants to drought in low and elevated CO_2. Global Change Biology 5(8): 857-867.

Wullschleger SD (1993) Biochemical limitations to carbon assimilation in C_3 plants - A retrospective analysis of the A/C_i curves from 109 species. J Exp Bot 44(5):907-920.

Ye Z, Suggett DJ, Robakowski P, Kang H (2013) A mechanistic model for the photosynthesis-light response based on the photosynthetic electron transport of photosystem II in C_3 and C_4 species. New Phytol 199(1):110–120.

Yin X, Van Der Putten PE, Driever SM, Struik PC (2016) Temperature response of bundle-sheath conductance in maize leaves. Journal of experimental botany 67(9): 2699-2714.

Yin X, Schapendonk AH, Struik PC (2018) Exploring the optimum nitrogen partitioning to predict the acclimation of C_3 leaf photosynthesis to varying growth conditions. Journal of experimental botany 70: 2435-2447.

Yin X, Struik PC (2012) Mathematical review of the energy transduction stoichiometries of C_4 leaf photosynthesis under limiting light. Plant, cell & environment 35(7): 1299-1312.

Yin X, Struik PC (2018) The energy budget in C_4 photosynthesis: insights from a cell-type-specific electron transport model. New Phytologist *218*(3): 986-998.

Yin X, Struik PC, Romero P, Harbinson J, Evers JB, Van Der Putten PE, Vos JAN (2009) Using combined measurements of gas exchange and chlorophyll fluorescence to estimate parameters of a biochemical C_3 photosynthesis model: a critical appraisal and a new integrated approach applied to leaves in a wheat (*Triticum aestivum*) canopy. Plant, Cell & Environment 32(5): 448-464.

Yin X, Sun Z, Struik PC, Van der Putten PE, Van Ieperen WIM, Harbinson J (2011) Using a biochemical C_4 photosynthesis model and combined gas exchange and chlorophyll fluorescence measurements to estimate bundle-sheath conductance of maize leaves differing in age and nitrogen content. Plant, cell & environment, 34(12): 2183-2199.

Zaehle S, Sitch S, Smith B, Hatterman F (2005) Effects of parameter uncertainties on the modeling of terrestrial biosphere dynamics. Global Biogeochemical Cycles 19(3): GB3020, doi:10.1029/2004GB002395.

Zhou H (2019) Selective pressures and evolutionary dynamics in hydraulic and photosynthetic systems of the C_3 and C_4 photosynthesis pathways in grasses. PhD thesis. University of Pennsylvania. https://repository.upenn.edu/edissertations/3398.

Zhou H, Akçay E, Helliker BR (2019) Estimating C_4 photosynthesis parameters by fitting intensive A/C_i curves. *Photosynthesis research*, 1-14 (doi: 10.1007/s11120-019-00619-8).

Zhou H, Helliker BR, Huber M, Dicks A, Akçay E (2018) C_4 photosynthesis and climate through the lens of optimality. Proceedings of the National Academy of Sciences 115: 12057-12062.

Supporting information

Fig. S1 Modeling results to show the effect of O_2 evolution on the assimilation rate of C_4 pathway.

Fig. S2 Modeling results of optimal V_{pmax}/V_{cmax} for C_4 under different environmental conditions.

Fig. S3 Sensitivity analysis of total nitrogen and PEPC stoichiometry on optimal J_{max}/V_{cmax} for C_3 and V_{pmax}/V_{cmax} C_4.

Table S1 The evolutionary models used for the phylogenetic analysis for photosynthetic properties evolutionary differences between C_3 and C_4 species.

Table S2 Phylogenetic analysis results for J_{max}/V_{cmax} for C_3 and C_4 species.

Table S3 Phylogenetic analysis results for V_{cmax} for C_3 and C_4 species.

Table S4 Phylogenetic analysis results for J_{max} for C_3 and C_4 species.

Table S5 Phylogenetic analysis results for total chlorophyll for C_3 and C_4 species.

Table S6 Phylogenetic analysis results for ETR/J for C_3 and C_4 species.

Table S7 Phylogenetic analysis results for chlorophyll a/chlorophyll b for C_3 and C_4 species.

Table S8 Phylogenetic analysis results for ETR for C_3 and C_4 species.

Table S9 Phylogenetic analysis results of evolutionary model fitting for V_{pmax} for C_4 species.

Table S10 Phylogenetic analysis results of evolutionary model fitting for Vpmax/Vcmax for C_4, C_3.

Table S11 Phylogenetic analysis results of evolutionary model fitting for J_{max}/V_{cmax} for C_3 and three C_4 subtypes.

Table S12 Phylogenetic analysis results of evolutionary model fitting for V_{cmax} for C_3 and three C_4 subtypes.

Table S13 Phylogenetic analysis results of evolutionary model fitting for J_{max} for C_3 and three C_4 subtypes.

Table S14 Phylogenetic analysis results of evolutionary model fitting for total chlorophyll for C_3 and three C_4 subtypes.

Table S15 Phylogenetic analysis results of evolutionary model fitting for ETR/J for C_3 and three C_4 subtypes.

Table S16 Phylogenetic analysis results of evolutionary model fitting for chlorophyll a/chlorophyll b for C_3 and three C_4 subtypes.

Table S17 Phylogenetic analysis results of evolutionary model fitting for ETR for C_3 and three C_4 subtypes.

Table S18 Phylogenetic analysis results of evolutionary model fitting for V_{pmax} for C_3 and three C_4 subtypes.

Table S19 Phylogenetic analysis results of evolutionary model fitting for V_{pmax}/V_{cmax} for C_3 and three C_4 subtypes.